CrossMark
click for updates

View Article Online
View Journal

Nanoscale

Accepted Manuscript

This article can be cited before page numbers have been issued, to do this please use: W. Yu, F. Li, H. wang, E. Alarousu, Y. Chen, B. Lin, L. Wang, M. N. Hedhili, Y. Li, K. Wu, X. Wang, O. F. Mohammed and T. T. Wu, *Nanoscale*, 2016, DOI: 10.1039/C5NR07758C.

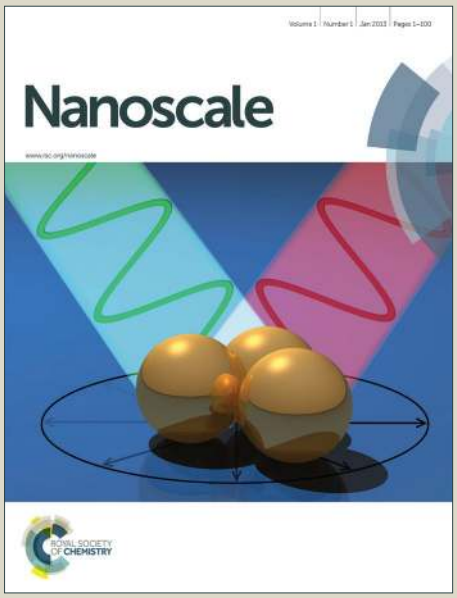

This is an *Accepted Manuscript*, which has been through the Royal Society of Chemistry peer review process and has been accepted for publication.

Accepted Manuscripts are published online shortly after acceptance, before technical editing, formatting and proof reading. Using this free service, authors can make their results available to the community, in citable form, before we publish the edited article. We will replace this *Accepted Manuscript* with the edited and formatted *Advance Article* as soon as it is available.

You can find more information about *Accepted Manuscripts* in the Information for Authors.

Please note that technical editing may introduce minor changes to the text and/or graphics, which may alter content. The journal's standard Terms & Conditions and the Ethical guidelines still apply. In no event shall the Royal Society of Chemistry be held responsible for any errors or omissions in this *Accepted Manuscript* or any consequences arising from the use of any information it contains.

ROYAL SOCIETY OF CHEMISTRY

www.rsc.org/nanoscale

Please do not adjust margins

View Article Online
DOI: 10.1039/C5NR07758C

Nanoscale

ARTICLE

Ultrathin Cu_2O as an efficient inorganic hole transporting material for perovskite solar cells

Received 00th January 20xx,
Accepted 00th January 20xx

DOI: 10.1039/x0xx00000x

www.rsc.org/

Weili Yu,[a,b] Feng Li,[a] Hong Wang,[a] Erkki Alarousu,[c] Yin Chen,[c,d] Bin Lin,[a] Lingfei Wang,[a] Mohamed Nejib Hedhili,[e] Yangyang Li,[a] Kewei Wu,[a] Xianbin Wang,[f] Omar F. Mohammed,[c] and Tom Wu [a,*]

We demonstrate that ultrathin P-type Cu_2O thin films fabricated by a facile thermal oxidation method can serve as a promising hole-transporting material in perovskite solar cells. Following a two-step method, inorganic-organic hybrid perovskite solar cells were fabricated and a power conversion efficiency of 11.0% was achieved. We find that the thickness and properties of Cu_2O layers must be precisely tuned in order to achieve the optimal solar cell performance. The good performance of such perovskite solar cells can be attributed to the unique properties of ultrathin Cu_2O, including high hole mobility, good energy level alignment with $CH_3NH_3PbI_3$, and longer lifetime of photo-excited carriers. Combining merits of low cost, facile synthesis, and high device performance, ultrathin Cu_2O films fabricated via thermal oxidation hold promise for facilitating the developments of industrial-scale perovskite solar cells.

Introduction,

The tremendous demands of clean, renewable and environment-friendly energy have stimulated the rapid developments of photovoltaic technologies, and particularly lead halide based perovskite solar cells attracted lots of recent interest.[1,2] Thanks to the compelling merits of perovskites such as low-cost processing, strong solar absorption, and long carrier diffusion lengths, power conversion efficiency (PCE) of perovskite solar cells has increased by several folds in a few years to about 20%.[3-10] In both planar and meso-porous structured perovskite solar cells, charge transporting materials play critical roles in the extraction and collection of photo-excited carriers. TiO_2 is routinely used as the electron transporting material (ETM) because of its suitable energy level for electron injection, high electron mobility, good stability and environmental friendliness.[11-13] It is more challenging to select appropriate hole transporting materials (HTMs) which are needed for effectively extracting holes from the perovskite layer while preventing electrons from recombination.[14-22]

Up to date, reported efficient HTMs include both organic and inorganic semiconductors.[14-23] Organic HTMs, such as 2,2',7,7'-tetrakis(N,N-di-p-meth-oxyphenylamine)-9,9'-spirobifluorene (spiro-OMeTAD), poly(3,4-ethylenedioxythiophene): polystyrene sulfonate (PEDOT:PSS), poly-3-hexylthiophene (P3HT) and poly-triarylamine (PTAA), suffer from high cost and low stability. Inorganic HTMs, particularly transition-metal oxides (such as WO_3, MoO_3, and V_2O_5), have merits such as low cost, chemical and thermal stability, as well as high work function.[23] However, to date the progress on developing inorganic HTMs for perovskite solar cells has been limited.[17,18,24] One main reason is that the thickness of transition-metal-oxide HTMs must be controlled within a few nanometers in order to avoid high series resistance,[23] but such ultrathin layers cannot provide complete coverage on perovskite layers with rough surfaces.[24-26] To solve this problem, a feasible strategy is to use the reversed solar cell structure, i.e., metal oxide HTMs are deposited on ITO substrate first, and then followed by the spin coating of the perovskite layers.[27-30] However, the limited choices of inorganic HTMs reported so far (**Table S1**) circumvents the developments of perovskite solar cells with structural variability and processing optimization. More environmentally friendly and efficient inorganic metal oxide semiconductors are in urgent needs for serving as HTMs in perovskite solar cells.

Cu_2O is a typical p-type semiconductor, which has been studied for decades due to its unique physical properties and applications in areas ranging from photoelectrochemistry[31] to magnetoelectrics[32] and superconductor[33]. A recent theoretical study proposed that Cu_2O might outperform other transition-

[a] *King Abdullah University of Science and Technology (KAUST), Material Science and Engineering, Thuwal 23955-6900, Saudi Arabia.*
[b] *School of Materials Science and Engineering, Changchun University of Science and Technology, Changchun 130022, P. R. China.*
[c] *King Abdullah University of Science and Technology (KAUST), Solar and Photovoltaics Engineering Research Center, Thuwal 23955-6900, Saudi Arabia.*
[d] *College of Chemistry and Chemical Engineering, Central South University, Changsha 410083, P. R. China.*
[e] *King Abdullah University of Science and Technology (KAUST), Imaging and Characterization Core Lab, Thuwal 23955-6900, Saudi Arabia.*
[f] *King Abdullah University of Science and Technology (KAUST), Nanofabrication Core Lab, Thuwal 23955-6900, Saudi Arabia.*
* Corresponding email: Tao.Wu@kaust.edu.sa
Electronic Supplementary Information (ESI) available: Experimental details, AFM images, XRD, hysteresis, XPS, EDAX, device stability and staticstics. See DOI: 10.1039/x0xx00000x

Published on 18 February 2016. Downloaded by King Abdullah Univ of Science and Technology on 23/02/2016 06:05:15.

Nanoscale Accepted Manuscript

Please do not adjust margins

View Article Online
DOI: 10.1039/C5NR07758C

Published on 18 February 2016. Downloaded by King Abdullah Univ of Science and Technology on 23/02/2016 06:05:15.

metal oxides including NiO as HTM in perovskite solar cells.[34] The unique merits of Cu_2O, such as low cost (**Table S2**) and environmental friendliness, make it a promising candidate for solar cell applications. Very recently, in a pioneering work, Zuo et al. fabricated Cu_2O and CuO films using in situ conversion of CuI film in NaOH aqueous solution.[35] However, the effect of Cu_2O layer thickness on the perovskite solar cell performance as well as the carrier dynamics have not been thoroughly investigated.

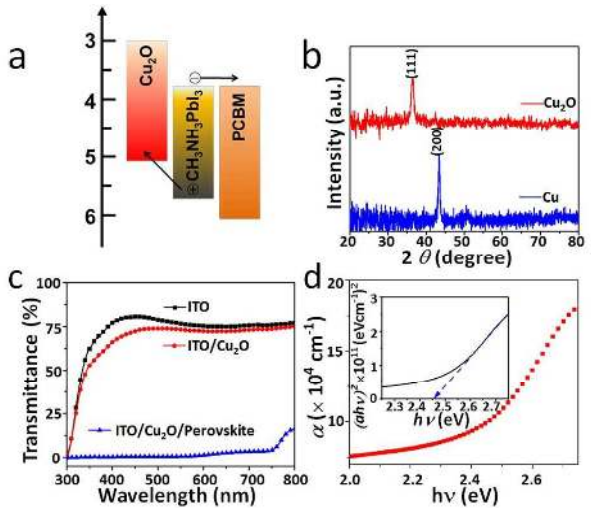

Fig.1 a) Energy alignment of the perovskite solar cells with Cu_2O as HTM and PCBM as ETM. b) XRD spectra of Cu and Cu_2O thin films. c) Transmittance spectra of ITO glass, ITO-Cu_2O and ITO-Cu_2O-perovskite samples. d) Absorption coefficient of the Cu_2O film and inset is the Tauc plot of the absorption data.

Here, we demonstrate that thermal oxidized ultrathin Cu_2O films can serve as an efficient HTM in perovskite solar cells. Ultrathin Cu_2O films were prepared via a facile process of Cu sputtering and controlled thermal oxidation, which is simple, suitable for large-scale processing and easy to control the layer thickness. Importantly, this synthesis route is suitable to optimize Cu_2O as the hole-transporting layer in perovskite solar cells. The optical and electrical properties of such ultrathin Cu_2O films were systematically characterized. The results of photoluminescence quenching and excitons relaxation dynamics of the perovskite/Cu_2O bilayers indicate efficient carrier transfer at the perovskite/Cu_2O interface. After optimizing the Cu_2O film thickness to 5 nm, which is probably the thinnest HTM reported to date, perovskite solar cells with a PCE of 11.0% were achieved under the AM1.5G solar illumination. Our findings strongly support Cu_2O as a promising inorganic HTM for industrial-scale perovskite solar cell applications.

Results and discussion

The work function of Cu_2O is around 5 eV,[36] which is lower than the valence band edge of $CH_3NH_3PbI_3$ (5.4 eV) [6] and favors the hole transfer at the interface (see **Figure 1a**). The XRD spectra of Cu layer (as prepared) and Cu_2O layer (after thermal oxidation at 250 °C in air for 1 hour) are presented in **Figure 1b**. The Cu film shows a peak at 43.9°, corresponding to the (111) plane of face-centered cubic structure. The Cu_2O film shows a peak at 36.9°, which can be assigned to the (111) diffraction of cubic-structured Cu_2O phase.[37] The ITO glass with 5 nm Cu_2O exhibits a color of slight brown. The AFM image of the Cu_2O film is presented in **Figure S1**. The root-mean square roughness (R_{rms}) of the Cu_2O-covered ITO film is 1.79 nm, which is slightly smoother than that of ITO surface (R_{rms}=1.96 nm). XPS characterizations also confirmed that most of the Cu ions in the films were in the 1+ valence state (Figure S2). These results indicate that the ultrathin Cu_2O films can be reliably achieved using the simple oxidation method.

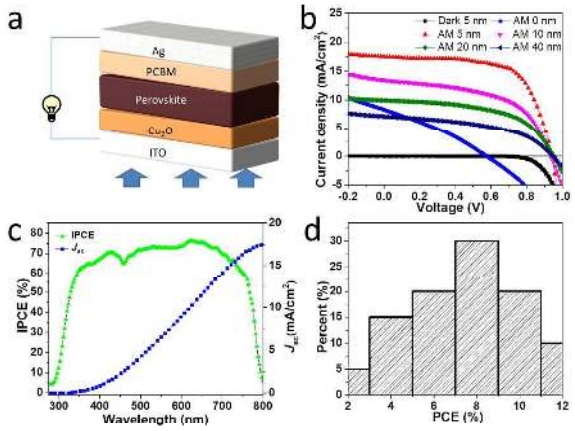

Fig.2 a) Structure of the perovskite solar cells. b) I-V performances of solar cells with different Cu_2O layer thicknesses in dark and under illumination (AM 1.5). c) IPCE spectra of the device with a Cu_2O layer of 5 nm. d) The statistical histogram plot of PCE for solar cells with 5 nm Cu_2O HTM.

Table 1. Dependence of solar cells performance on the Cu_2O layer thickness.

Cu_2O thickness (nm)	J_{sc} (mA/cm^2)	V_{oc} (V)	FF (%)	PCE (%)	R_s (Ohm*cm^2)	R_{sh} (Ohm*cm^2)
0	8.3	0.576	30.7	1.47	47.9	54.9
5	17.5	0.952	66.2	11.03	7.6	555.6
10	13.3	0.947	57.4	7.20	13.3	568.2
20	9.9	0.941	50.3	4.69	19.1	1250.0
40	7.1	0.940	45.6	3.04	31.4	862.6

The Cu_2O layers must be as thin as possible because thick Cu_2O layers will suffer from poor transmittance and high resistance. **Figure 1c** shows the transmittance spectra of ITO with and without Cu_2O. For bare ITO glass, the transmittance is above 75% when wavelength is longer than 370 nm. After covering 5 nm Cu_2O, the transmittance of ITO glass decreases slightly, but it remains above 75% at wavelength above 420 nm. The absorption coefficient α of Cu_2O layer is shown in **Figure 1d**, which was calculated according to the following formula:

$$\alpha = -\ln T/d \quad (1)$$

Nanoscale Accepted Manuscript

This journal is © The Royal Society of Chemistry 20xx

Please do not adjust margins
View Article Online
DOI: 10.1039/C5NR07758C

Published on 18 February 2016. Downloaded by King Abdullah Univ of Science and Technology on 23/02/2016 06:05:15.

where T is the transmittance and d is the film thickness. Figure 1d indicates that the Cu_2O layer has high absorption coefficient (> 10^5) in the visible range, especially for light with wavelength below 500 nm. Thus, the Cu_2O layer should be as thin as possible to decrease the absorption. The dependence of transmittance on the Cu_2O thickness is shown In **Figure S3**. From the Tauc plots shown in the inset of Figure 1d, the bandgap (E_g) of Cu_2O layer is deduced from:

$$\alpha^n = B(hv - E_g) \quad (2)$$

where hv is the energy of incident photons and B is a constant. A good fitting was achieved with n = 2, indicating a direct bandgap nature of the Cu_2O film.[37] According to the Eq.(2), we calculated E_g of Cu_2O layer as 2.24 eV, which is slightly higher than the value reported in literature for bulk Cu_2O,[36] which may be related to the quantum confinement in such ultrathin Cu_2O films.

The solar cell structure is presented in **Figure 2a**. Ultrathin Cu_2O layers between ITO glass and perovskite served as the HTM, and $PC_{61}BM$ was introduced as the ETM and hole blocking layer. Compared to the mesoporous perovskite solar cells, planar ones are easier to fabricate and to scale up.[8,9] The perovskite layers with a thickness of 400 nm were prepared using the two-step method. A 60 °C pre-heated PbI_2 solution (1 M, N, N-dimethylformamide) was first spin-coated on ITO/Cu_2O. After several minutes of drying, the yellow colored films were dipped into CH_3NH_3I solution (10 mg/l, isopropanol) for 30 s to convert PbI_2 into $CH_3NH_3PbI_3$, which was accompanied by the change of color from yellow to dark brown. The formation of the perovskite phase was further confirmed by the XRD spectra (**Figure S4**). We also tried one-step method by spin-coating the mixed solution of $PbCl_2$ and CH_3NH_3I onto ITO/Cu_2O, but no pure perovskite phase was achieved after annealing at 100 °C, which might be related to the surface properties of Cu_2O films.[38-40] Further optimization of device performance was thus focused on using the two-step method since the residual PbI_2 provides the beneficial effect of passivation.[41]

Figure 2b presents the current density-voltage (*J-V*) curves of the perovskite solar cells using Cu_2O as the HTM. We observed significant dependence of the solar cell performance on the thickness of Cu_2O layers. PCE, fill factor (FF) and the short-circuit current density (J_{sc}) decrease with increasing Cu_2O layer thickness (**Table 1**). This can be attributed to the increases of absorption (**Figure S3**) and series resistance associated with thicker Cu_2O layers. When Cu_2O layer was 5 nm, a champion device with a PCE of 11.0% was achieved, with a J_{sc} of 17.5 mA/cm^2, an open-circuit voltage (V_{oc}) of 0.95 V and a FF of 66.2%. Cu_2O layers thinner than 5 nm resulted in poor coverage and high leakage current. The observed V_{oc} of 0.95 V is much higher than that of the solar cells with CuI HTM (0.55 V),[18] which presumably can be attributed to the lower valence band of Cu_2O in reference to CuI. Comparing with the state-of-the-art inorganic HTMs reported so far (see **Table S1**), Cu_2O is clearly a very competitive candidate. The incident photon-to-current efficiency (IPCE) of the device is shown in **Figure 2c**, which is featured with a high platform between 350 nm to 700 nm with the maximum of 78% at 620 nm. The integrated current density was calculated to be 17.6 mA/cm^2, which is consistent with the measurement results in Figure 2b.

Anomalous photocurrent hysteresis was observed during the current-voltage measurements (see **Figure S5**). With voltage scanning in the direction of forward-bias (FB) to short-circuit (SC) conditions, the solar cell showed a higher FF (66.2%) and lower J_{sc} (17.50 mA/cm^2) than those of scanning in the SC-to-FB direction (FF: 58.0%; J_{sc}: 18.47 mA/cm^2), corresponding to a higher PCE (11.0%) for FB-to-SC than that for SC-to-FB (10.1%). The differences in J_{sc} and FF were likely due to the migration of defects near the perovskite/charge

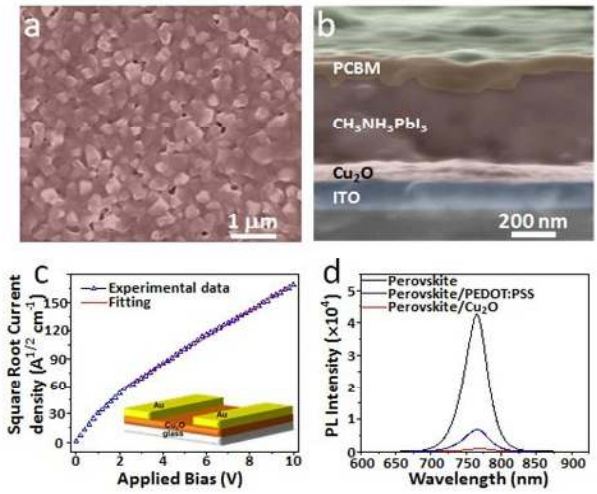

Fig. 3 a) Top-view SEM image of the $Cu_2O/CH_3NH_3PbI_3$ perovskite layer. b) Cross-sectional SEM image of the perovskite solar cell. c) SCLC measurement of the Cu_2O layer. Inset shows the measurement configuration. d) Steady state photoluminescence of the perovskite layers fabricated on glass, PEDOT:PSS/glass and Cu_2O/glass substrates.

transporter interfaces.[42-44] Charges trapping and polarization effect could also contribute to the slow dynamics of transport measurements.[44] Nevertheless, by applying a bias at the maximum power point (0.74 V), we confirmed that the PCE of 11% could be reliably achieved.

The stability of perovskite solar cells with Cu_2O as HTM was also characterized and the results were shown in **Figure S6**. Interestingly, J_{sc} reached the peak value only after several days of storage and measurements, which might be caused by the light soaking effect.[45] The PCE of solar cells without encapsulation kept going down during the stability test, which is mainly a result of the decreases of V_{oc} and FF. The underlying reason could be the oxidation and degradation of perovskite due to the penetration of oxygen and moisture.[46] The histogram plot of PCE for solar cells is shown in **Figure 2d**. About half of the devices exhibited PCE above 8%, indicating the consistent high performance of Cu_2O as HTM. The statistical information of J_{sc}, V_{oc} and FF of these perovskite solar cells are summarized in **Figure S7**.

Performance of perovskite solar cells, especially photocurrent and FF, is closely related to the thickness and morphology of the perovskite layers.[6,7] In comparison with the

Nanoscale Accepted Manuscript

Please do not adjust margins

View Article Online
DOI: 10.1039/C5NR07758C

Published on 18 February 2016. Downloaded by King Abdullah Univ of Science and Technology on 23/02/2016 06:05:15.

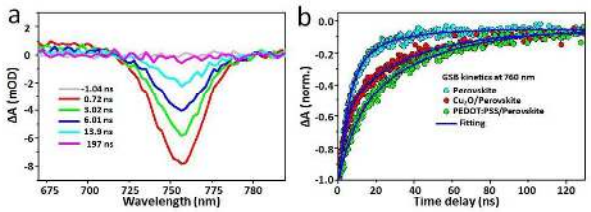

Fig. 4 a) Transient absorption spectra of perovskite on different substrates at time delays from -1 ns to 197 ns. b) Kinetics of GSB recovery at 760 nm for perovskite layers on different substrates.

mesoporous structured solar cells, the planar ones offer more freedom in controlling the device size and film morphology.[8,9] As shown in the SEM image (**Figure 3a**), the perovskite grains appear to be uniform, with an average size of approximately 350 nm. Such large grain sizes are favorable for transporting and collecting photo-generated carriers, while suppressing the defect-induced carrier recombination at the grain boundaries.[9]

As shown in **Figure S8**, the energy dispersive X-ray (EDAX) measurements confirmed the presence of all elements in the layers, including Cu. The cross-section SEM image of the solar cell (**Figure 3b**) indicates that all the layers appear to be uniform and the perovskite layer was fully covered by PCBM. The thicknesses of the perovskite and the PCBM layers are approximately 400 nm and 50 nm, respectively. Importantly, PCBM infiltrated between perovskite grains, which facilitates effective charge generation and transportation.

Carrier mobility of HTM plays a key role in achieving highly efficient solar cells because it helps reduce the series resistance and enhance the FF. As shown in **Figure 3c**, the current-voltage curve measured on a Cu_2O layer can be described by the space-charge-limited current (SCLC) model:

$$J = \frac{9}{8}\varepsilon_0\varepsilon\mu\frac{V^2}{d^3} \qquad (3)$$

where ε_0 is the permittivity of free space (8.85×10^{-12} Fm^{-1}), ε is the dielectric constant of Cu_2O (=7.5), μ is the charge carrier mobility, and d is the film thickness (40 nm). From the data fitting, we calculated the hole mobility of Cu_2O layer to be 0.49 $cm^2 \cdot V^{-1} \cdot s^{-1}$, which is much higher than those of organic counterparts like spiro-MeOTAD and PEDOT:PSS.[47,48] In comparison, the carrier mobility of spiro-MeOTAD increased from 1.6×10^{-4} $cm^2 \cdot V^{-1} \cdot s^{-1}$ to 1.6×10^{-3} $cm^2 \cdot V^{-1} \cdot s^{-1}$ after doping with lithium salts,[47] and the carrier mobility of PEDOT:PSS can reach 1.28×10^{-2} $cm^2V^{-1}s^{-1}$ after annealing.[48]

To understand the role of Cu_2O layer in perovskite solar cells and the properties of interfaces, we performed steady-state photoluminescence (PL) measurements. **Figure 3d** presents the steady state photoluminescence of perovskite and perovskite deposited on various HTMs. Under the same conditions, all samples exhibit a PL peak at 760 nm; however, comparing to pure perovskite film, the PL summit values of perovskite are largely reduced when interfacing with HTM layers. Such a dramatic PL quenching is particularly interesting in solar cell research because it could be caused by the significantly enhanced charge carrier extraction from the perovskite layer to the electrode. Especially, The PL data shows that less than 2% of the PL peak height at 760 nm remained when the Cu_2O layer was introduced as HTM, which is much better than that of PEDOT:PSS (16% left). Since the Cu_2O thin film has the high carrier mobility and the narrow barrier between the valance band of perovskite and the work function of Cu_2O (**Figure 3c**,), fast carriers transfer from perovskite to Cu_2O is thermodynamically favored. The observed significant PL quenching unambiguously suggests Cu_2O as an effective HTM for perovskite solar cells.

To further understand the role of Cu_2O layer in working solar cell devices, we utilized nanosecond transient absorption (ns-TA) spectroscopy to investigate the excitons relaxation dynamics of perovskite/Cu_2O bilayers. For comparison, the same experiment was performed on a sample with Cu_2O replaced with PEDOT:PSS/glass. As a reference, a sample of perovskite layer fabricated on glass without HTM was also measured. As shown in **Figure 4a**, the photobleaching band of perovskite layer at 760 nm is observed, which is consistent with the steady-state PL quenching experiment. The kinetic decay traces of photobleaching features are presented in **Figure 4b**, which are fitted to a double exponential function. The decay component of τ_1 and τ_2 were ascribed to bimolecular recombination and free carriers recombination, respectively (**Table S3**).[49-52] Comparison between these three samples gives valuable insights on the role of HTMs in photovoltaic operations. The faster decay component τ_1 of perovskite film (3.88 ns) on Cu_2O is smaller than those of samples on glass (5.51 ns) and PEDOT:PSS/glass (9.11 ns), suggesting a faster bimolecular recombination and stronger electronic coupling between perovskite and Cu_2O layer. The slower time constant τ_2 is related to the excited-state decay and carrier recombination dynamics in the perovskite layers.[49,50] τ_2 of perovskite/Cu_2O sample is approximately 50% higher than that of perovskite on glass, indicating that the photo-excited carriers in the perovskite solar cells with Cu_2O HTM have a longer lifetime and more opportunities to be collected by the electrodes. When the time delay is above 100 ns, Cu_2O showed very similar performance as PEDOT:PSS, the well-known HTM for solar cells. To corroborate this observation, we fabricated and measured a solar cells using PEDOT:PSS as HTM. This device showed an efficiency of 12.1% (**Figure S9**), comparable to the Cu_2O device, confirming that Cu_2O is a very competitive HTM for perovskite solar cells.

Conclusions

In summary, we demonstrated the application of ultrathin p-type Cu_2O derived from simple oxidization as a promising inorganic HTM in perovskite solar cells. The scarcity of high-performance p-type inorganic semiconductors makes Cu_2O a valuable addition to the family of charge transporters for perovskite photovoltaic applications. Our experiments revealed that both the thickness and the properties of Cu_2O layers must be carefully tailored in order to achieve the optimal solar cell performance. Using the two-step method to prepare the perovskite layer, PCE of 11.0% was achieved under the AM 1.5 G illumination with ultrathin (5 nm) Cu_2O films as HTM. The ultrathin nature of the Cu_2O film helps in reducing

Nanoscale Accepted Manuscript

This journal is © The Royal Society of Chemistry 20xx

View Article Online
DOI: 10.1039/C5NR07758C

Published on 18 February 2016. Downloaded by King Abdullah Univ of Science and Technology on 23/02/2016 06:05:15.

the material consumption and manufacture cost in large-scale production of perovskite solar cells. The high performance of such perovskite solar cells can be attributed to the unique properties of the prepared Cu_2O layers, including high hole mobility, well-matched energy levels, and long lifetime of photo-excited carriers. Combining merits of low cost, facile synthesis, and high device performance, Cu_2O holds promise for facilitating the developments of industrial-scale perovskite solar cells.

Experimental details

Synthesis

Methylammonium iodide (CH_3NH_3I) was prepared according to previous report [32]. Briefly, 27.86 ml methylamine (40% in methanol) and 30ml hydroiodic acid (57 wt% in water) were mixed at 0 °C and stirred for 2 h. The precipitate was recovered by evaporation at 50 °C for 1 h. The product was washed with diethyl ether three times and finally dried at 60 °C in a vacuum oven for 24 h. lead iodide (PbI_2) was purchased from Aldrich and was recrystallized twice before use.

Solar Cell Fabrication

A thin layer of Cu was first sputtered onto ITO glass (Equipment Support Co., Cambridge, England), then the Cu_2O phase was achieved via annealing the ITO/Cu on a hotplate in air at 250 °C for an hour. The film thickness was carefully controlled by the sputtering time. The substrate was then transferred into glove box immediately for following process. The perovskite layer was fabricated by a two-step method onto ITO/Cu_2O substrates. PbI_2 solution (0.46 g/ml in DMF) was spin-coated at 2000 rpm for 45 s. Then the PbI_2 film was annealed at 100 °C on hotplate for 15 min. After cooling down, the devices were dipped into MAI solution (10 mg/ml in iso-propanol) for 30 s. After washing with iso-propanol, the devices were heated at 70 °C for 30 min and then at 130 °C for 10 min. A layer of Phenyl-C61-butyric acid methyl ester (PCBM, 15 mg/ml in chlorobenzene) was then spin coated on top of the perovskite film. Finally, an Ag layer (120 nm) was evaporated in vacuum as top electrodes. For PL or transient absorption measurements, the samples were prepared as mentioned above except that no Ag layer was needed. The perovskite films were finally covered by a poly(methyl methacrylate) (PMMA*)* layer via spin coating a 10 wt% chlorobenzene solution at 2000 rpm for 30s.

Characterizations

UV-Vis spectra were collected using a JASCO V-670 spectrophotometer equipped with an integrating sphere. X-ray diffraction (XRD) was performed at room temperature using an X-ray diffractometer (D8 Discover, Bruker). Atomic force microscope (AFM) characterization was conducted on a Bruker's Dimension Icon system. XPS measurements were carried out in a Kratos Axis Ultra DLD spectrometer equipped with a monochromatic Al Kα X-ray source (hν = 1486.6 eV) operating at 150 W. The spectra were recorded using an aperture slot of 300 µm x 700 µm. The survey and high-resolution spectra were collected at fixed analyser pass energies of 160 eV and 20 eV, respectively. Samples were mounted in the floating mode in order to avoid differential charging**.** The current density-voltage (J-V) measurements were conducted on a OAI Trisol tester system combined with a Keithley 2400 source-meter. The light intensity was calibrated to be 100 mW/cm^2 before measurements. The incident photon-to-current efficiency (IPCE) of the device was measured by using an Oriel IQE200 quantum efficiency measurement system.[53] The morphology of samples was investigated using an FEI Nova Nano 630 scanning electron microscopy (SEM). Photoluminescence measurement was conducted on a Horiba Armis equipment and the excitation light source was 632 nm laser. For the nanosecond transient absorption spectroscopy, a few µJ of pulse energy as the fundamental output from a Ti: Sapphire femtosecond regenerative amplifier (800 nm, 35 fs FWHM, 1 kHz, Newport Spectra-Physics) was used to generate pump and probe beams. By introducing the fundamental beams into an optical parametric amplifier (Light Conversion Ltd), we could select a certain wavelength from the tunable output (240–2600 nm) as the pump pulses, whereas light continuum probe pulses were obtained by focusing the fundamental beams onto a 2-mm-thick sapphire plate (contained in an Ultrafast System LLC spectrometer). The pump and probe pulses overlapped by a small angle of less than 5° on the perovskite samples. The transmitted probe light from the samples was collected and focused on the broadband VIS-NIR detector for recording the time-resolved excitation induced difference spectrum (ΔOD). Details of the TA setup were published elsewhere.[54]

Acknowledgements

This work was supported by King Abdullah University of Science and Technology (KAUST). Dr. W. Yu acknowledges the support from the National Natural Science Foundation of China (NSFC 21404015).

Notes and references

1 S. Kazim, M. K. Nazeeruddin, M. Gratzel, S. Ahmad, *Angew. Chem. Int. Ed.,* 2014, **53**, 2812.
2 M. A. Green, A. Ho-Baillie, H. J. Snaith, *Nat. Photon.*, 2014, **8**, 506.
3 A. Kojima, K. Teshima, Y. Shirai, T. Miyasaka, *J. Am. Chem. Soc.*, 2009, **131**, 6050.
4 J.-H. Im, C.-R. Lee, J.-W. Lee, S.-W. Park, N.-G. Park, *Nanoscale,* 2011, **3**, 4088.
5 H.-S. Kim, C.-R. Lee, J.-H. Im, K.-B. Lee, T. Moehl, A. Marchioro, S.-J. Moon, R. Humphry-Baker, J.-H. Yum, J. E. Moser, M. Graetzel, N.-G. Park, *Sci. Rep.*, 2012, **2**, 591.
6 M. M. Lee, J. Teuscher, T. Miyasaka, T. N. Murakami, H. J. Snaith, *Science,* 2012, **338**, 643.
7 H. Zhou, Q. Chen, G. Li, S. Luo, T.-b. Song, H.-S. Duan, Z. Hong, J. You, Y. Liu, Y. Yang, *Science,* 2014, **345**, 542.
8 D. Liu and T. L. Kelly, *Nat. Photon.,* 2014, **8**, 133.
9 J.-H. Im, I.-H. Jang, N. Pellet, M. Graetzel, N.-G. Park, *Nat. Nanotechnol.*, 2014, **9**, 927.
10 N. J. Jeon, J. H. Noh, W. S. Yang, Y. C. Kim, S. Ryu, J. Seo, S. I. Seok, *Nature*, 2015, **517**, 476.

Nanoscale Accepted Manuscript

View Article Online
DOI: 10.1039/C5NR07758C

Published on 18 February 2016. Downloaded by King Abdullah Univ of Science and Technology on 23/02/2016 06:05:15.

11 A. Hagfeldt, G. Boschloo, L. Sun, L. Kloo, H. Pettersson, *Chem. Rev.,* 2010, **110**, 6595.
12 X. Chen, S. S. Mao, *Chem. Rev.*, 2007, **107**, 2891.
13 A. Bera, K. Wu, A. Sheikh, E. Alarousu, O. F. Mohammed, T. Wu, *J. Phys. Chem. C,* 2014, **118**, 28494.
14 H. Wang, A. D. Sheikh, Q. Feng, F. Li, Y. Chen, W. Yu, E. Alarousu, C. Ma, M. A. Haque, D. Shi, Z.-S. Wang, O. F. Mohammed, O. M. Bakr, T. Wu, *ACS Photon.*, 2015, **2**, 849.
15 J. H. Heo, S. H. Im, J. H. Noh, T. N. Mandal, C.-S. Lim, J. A. Chang, Y. H. Lee, H.-j. Kim, A. Sarkar, Md. K. Nazeeruddin, M. Graetzel, S. I. Seok, *Nat. Photon.*, 2013, **7**, 486.
16 N. J. Jeon, J. Lee, J. H. Noh, M. K. Nazeeruddin, M. Graetzel, S. I. Seok, *J. Am. Chem. Soc.,* 2013, **135**, 19087.
17 P. Qin, S. Tanaka, S. Ito, N. Tetreault, K. Manabe, H. Nishino, M. K. Nazeeruddin, M. Gratzel, *Nat. Commun.*, 2014, **5**, 3834.
18 J. A. Christians, R. C. M. Fung, P. V. Kamat, *J. Am. Chem. Soc.*, 2014, **136**, 758.
19 W. Yan, Y. Li, Y. Li, S. Ye, Z. Liu, S. Wang, Z. Bian, C. Huang, *Nano Energy*, 2015, **16**, 428.
20 Q. Wang, C. Bi, J. Huang, *Nano Energy*, 2015, **15**, 275.
21 S. Ye, W. Sun, Y. Li, W. Yan, H. Peng, Z. Bian, Z. Liu, C. Huang, *Nano Lett.*, 2015, **15**, 3723.
22 U. Bansode, R. Naphade, O. Game, S. Agarkar, S. Ogale, *J. Phys. Chem. C,* 2015, **119**, 9177.
23 J. Meyer, S. Hamwi, M. Kröger, W. Kowalsky, T. Riedl, A. Kahn, *Adv. Mater.*, 2012, **24**, 5408.
24 Y. Zhao, A. M. Nardes, K. Zhu, *Appl. Phys. Lett.*, 2014, **104**, 213906.
25 P. Gao, M. Gratzel, M. K. Nazeeruddin, *Energy Environmen. Sci.*, 2014, **7**, 2448.
26 Kazim, M. K. Nazeeruddin, M. Gratzel, S. Ahmad, *Angew. Chem. Int. Ed.*, 2014, **53**, 2812.
27 J. Y. Jeng, K. C. Chen, T. Y. Chiang, P. Y. Lin, T. D. Tsai, Y. C. Chang, T. F. Guo, P. Chen, T. C. Wen, Y. J. Hsu, *Adv. Mater.*, 2014, **26**, 4107.
28 Z. Zhu, Y. Bai, T. Zhang, Z. Liu, X. Long, Z. Wei, Z. Wang, L. Zhang, J. Wang, F. Yan, S. Yang, *Angew. Chem. Int. Ed.*, 2014, **53**, 12571.
29 M. D. Irwin, D. B. Buchholz, A. W. Hains, R. P. H. Chang, T. J. Marks, *PNAS*, 2008, **105**, 2783.
30 K.C. Wang, J.Y. Jeng, P.S. Shen, Y.C. Chang, E. W.G. Diau, C.H. Tsai, T.Y. Chao, H.C. Hsu, P.Y. Lin, P. Chen, T.F. Guo, T.C. Wen, *Sci. Rep.*, 2014, **4**, 4756.
31 A. Paracchino, V. Laporte, K. Sivula, M. Grätzel, E. Thimsen, *Nat. Mater.,* 2011, **10**, 456.
32 Y. Kitagawa, Y. Hiraoka, T. Honda, T. Ishikura, H. Nakamura, T. Kimura, *Nat. Mater.*, 2010, **9**, 797.
33 O. Chmaissem, J. D. Jorgensen, S. Short, A. Knizhnik, Y. Eckstein, H. Shaked, *Nature,* 1999, **397**, 45.
34 Y. Wang, Z. G. Xia, J. Liang, X. W. Wang, Y. M. Liu, C. Liu, S. D.Zhang, H. Zhou, *Semicond. Sci. Tech.,* 2015, **30**, 054004.
35 C. Zuo, L. Ding, *Small* 2015, DOI: 10.1002/smll.201501330.
36 W.-Y. Yang, S.-W. Rhee, *Appl. Phys. Lett.,* 2007, **91**, 232907.
37 Y. Nakano, S. Saeki, T. Morikawa, *Appl. Phys. Lett.*, 2009, **94**, 022111.
38 J. Li, Z. Mei, L. Liu, H. Liang, A. Azarov, A. Kuznetsov, Y. Liu, A. Ji, Q. Meng, X. Du, *Sci. Rep.*, 2014, **4**, 7240.
39 K.D. Liang, C.H. Huang, C.C. Lai, J.S. Huang, H.W. Tsai, Y.C. Wang, Y.C. Shih, M.T. Chang, S.C. Lo, Y.L. Chueh, *ACS Appl. Mater. Interfaces*, 2014, **6**, 16537.
40 M. M. Tavakoli, L. Gu, Y. Gao, C. Reckmeier, J. He, A. L. Rogach, Y. Yao, Z. Fan, *Sci. Rep.*, 2015, **5**, 14083.
41 D. H. Cao, C. C. Stoumpos, C. D. Malliakas, M. J. Katz, O. K. Farha, J. T. Hupp, M. G. Kanatzidis, *APL Mater.*, 2014, **2**, 091101.
42 E. L. Unger, E. T. Hoke, C. D. Bailie, W. H. Nguyen, A. R. Bowring, T. Heumueller, M. G. Christoforo, M. D. McGehee, *Energy Environ. Sci.*, 2014, **7**, 3690.
43 X. Zheng, B. Chen, C. Wu, S. Priya, *Nano Energy*, 2015, **17**, 269.
44 R. S. Sanchez, V. Gonzalez-Pedro, J.-W. Lee, N.-G. Park, Y. S. Kang, I. Mora-Sero, J. Bisquert, *J. Phys. Chem. Lett.*, 2014, **5**, 2357.
45 C. E. Small, S. Chen, J. Subbiah, C. M. Amb, S.-W. Tsang, T.-H. Lai, J. R. Reynolds, F. So, *Nat. Photon.*, 2012, **6**, 115.
46 A. D. Sheikh, A. Bera, M. A. Haque, R. B. Rakhi, S. D. Gobbo, H. N. Alshareef, T. Wu, *Sol. Energy Mater. Sol. Cells*, 2015, **137**, 6.
47 H. J. Snaith, M. Grätzel, *Appl. Phys. Lett.*, 2006, **89**, 262114.
48 S. A. Rutledge, A. S. Helmy, *J. Appl. Phys.,* 2013, **114**, 133708.
49 Q. Chen, H. Zhou, T.-B. Song, S. Luo, Z. Hong, H.-S. Duan, L. Dou, Y. Liu, Y. Yang, *Nano Lett.,* 2014, **14**, 4158.
50 L. Zuo, Z. Gu, T. Ye, W. Fu, G. Wu, H. Li, H. Chen, *J. Am. Chem. Soc.*, 2015, **137**, 2674.
51 S. D. Stranks, G. E. Eperon, G. Grancini, C. Menelaou, M. J. P. Alcocer, T. Leijtens, L. M. Herz, A. Petrozza, H. J. Snaith, *Science*, 2013, **342**, 341.
52 G. Xing, N. Mathews, S. Sun, S. S. Lim, Y. M. Lam, M. Graetzel, S. Mhaisalkar, T. C. Sum, *Science*, 2013, **342**, 344.
53 M. I. Saidaminov, A. L. Abdelhady, B. Murali, E. Alarousu, V. M. Burlakov, W. Peng, I. Dursun, L. Wang, Y. He, G. Maculan, A. Goriely, T. Wu, O. F. Mohammed, O. M. Bakr, *Nature Comm.* 2015, **6**, 7586.
54 O. F. Mohammed, D. Xiao, V. S. Batista, E. T. J. Nibbering, *J. Phys. Chem. A*, 2014, **118**, 3090.

Nanoscale Accepted Manuscript

This journal is © The Royal Society of Chemistry 20xx